# QSO colors in the proposed GAIA photometric systems

*J.-F. Claeskens, P. Royer and J. Surdej*

Institute of Astrophysics and Geophysics
Liège University, Belgium

---

## 1 Introduction

About 500,000 quasi stellar extragalactic sources (called quasars or QSOs) with magnitude $V \leqslant 20$ and galatic latitude $|b| > 25°$ will be detected by GAIA.

Such a large and *complete* catalog of QSOs will not only represent a gold mine to study the evolution of quasars and the large scale structures they might trace but it will also provide a dense grid of distant background sources ($\simeq$ 20/ square degree). Their spectra may then be used to search for absorbing signatures by intergalactic clouds or by galactic haloes lying on the lines-of-sight; these sources will also help in determining the inertial frame against which the motion of the galactic stars will be measured. But the most interesting use of this huge set of quasars certainly goes through *gravitational lensing* effects. Indeed, the latter constitute a very powerful tool, not only to investigate the fate and the size of the Universe as a whole (constrained by the number of lenses in a complete sample of QSOs), but also to study the astrophysical properties of the remote galaxies acting as gravitational lenses (such as their mass, their extinction law, etc...) and to explore the structure of the background sources (accretion disk, central engine, etc.) through microlensing studies.

Thanks to its high angular resolution, GAIA is expected to detect, some 1,000 quasars with multiple images produced by foreground galaxies, i.e. with angular separations typically smaller or equal to 3 arcsec. This is about 20 times the number of presently known gravitational lenses and this will be the most complete sample.

In order to reach these scientific goals, the first step to be fullfiled is the *identification* of *all* the quasars among the billions of pointlike sources which will be detected by GAIA. This identification will rely on four properties of QSOs: their negligible parallax, their negligible proper motion, their photometric variability (every quasar is variable, at least at the 0.01 mag level) and their peculiar colour indices. The present preliminary study is focused on the last property: its aim is to explore QSO colors in the different photometric systems proposed so far for GAIA (namely the 1F, 3G and 2A systems). The distance of the QSOs to the stellar locus in the multidimensional color space as a function of redshift and the ability to retrieve

the photometric QSO redshift up to V = 20 will be considered.

## 2 Modeling colors of QSOs and stars

The UV-optical spectrum of a QSO consists in the superposition of a powerlaw continuum ($F_\nu \propto \nu^{-\alpha}$, or $F_\lambda \propto \lambda^{\alpha-2}$) and of strong broad emission-lines, like $Ly_\alpha$ (1216Å), CIV (1549Å), CIII] (1909Å), MgII (2798Å), $H_\alpha$ (6563Å). The situation is complicated by two facts. First, the intrinsic emission spectrum is *redshifted* and the emission lines are *broadened* accordingly by the cosmological factor $(1 + z_q)$, where $z_q$ is the redshift of the quasar. Second, the spectrum is *absorbed* on the blue side of the $Ly_\alpha$ line by intergalactic hydrogen clouds lying at any redshift $z_c \leqslant z_q$ (those clouds are called Lyman forest (LF), Lyman limit systems (LLS) or damped $Ly_\alpha$ (DLA) systems, according to the hydrogen column density). The absorption is of course stronger in the spectra of high redshift QSOs. The absorption region can be divided into 3 intervals in the referential frame of the source: zone A [1216 - 1025Å], which can only be affected by $Ly_\alpha$ absorption lines; zone B [1025 - 912Å], which can also be affected by $Ly_\beta$ absorption lines; zone C [$\leqslant$ 912Å] which can also be affected by the other Ly lines and by continuum absorption. While the absorption may be statistically studied from observations in the two first intervals, it is highly model and/or line-of-sight dependent in the last interval, since the continuum absorption of one individual thick cloud may be very strong.

In summary, since QSO colors are strongly sensitive to the emission lines and to the amount of absorbing gas located along the line-of-sight, they will primarily depend on $z_q$. However, they also slightly depend on the exact slope of the continuum and on the relative strengths of the emission-lines.

The QSO composite spectrum we used as a template in our simulations has been built from *observations* as specified in Table 1. The estimation of absorption along the line-of-sight comes from *observations* by Irwin et al. (1991) and Zuo & Lu (1993) in zone A, from *observations* by Warren, Hewett and Osmer (1994) in zone B and from three different *models* of absorber in zone C: 1- LF; 2- LF+LLS; 3- absorption by 10 magnitudes (Models 1 +2: Møller & Jakobsen (1990), Møller & Warren (1991), Warren et al. (1994) and Giallongo & Trevese (1990)).

In the present study, the QSO colors are derived by integrating the composite spectrum through the different filters, whose transmission curves have been multiplied by the adequate CCD response curve. The colors are given in instrumental magnitudes, with no color correction.

Table 1: Contributions to the composite QSO spectrum

| $\lambda$ range (Å) | $\alpha$ | Reference |
|---|---|---|
| 310 – 1050 | -1.96 | Zheng et al. (1997) |
| 1050 – 2000 | -0.99 | Zheng et al. (1997) |
| 2000 – 6000 | -0.32 | Francis et al. (1991) |
| 6000 – 8000 | -0.32 | Cristiani & Vio (1990) |

Table 2: Stellar types with contaminating colors

| Type | Log $g$ | [Fe/H] | $T_{eff}(K)$ |
|---|---|---|---|
| Disk MS | 4 | 0 | 3,500–7,000 |
| Halo MS | 4 | -1.5 | 3,500–7,000 |
| Halo Giants | 3 | -1.5 | 3,500–7,000 |
| HB | f($T_{eff}$) | 0.5 | 10,000 – 30,000 |
| sd OB | 5 | 0 | 20,000 – 50,000 |
| White dwarfs | 8.5 | - | 7,000 – 80,000 |

In order to compare the QSO colors with the stellar colors, we have also integrated synthetic spectra of non degenerated stars with metallicity [Fe/H]$> -3$ given in Kurucz's ATLAS 9 atmosphere models (Kurucz 1992), and of white dwarfs (Koester 1999). The most contaminating stellar types present at relatively high galactic latitude are summarized in Table 2, together with their astrophysical properties.

# 3 Analysis of the QSO colors

In this section, we discuss three aspects of QSO colors. First, we describe some color-color diagrams, then we present, as a function of redshift, the shortest distance in the multidimensional color space between QSO colors and the stellar locus and finally, we show some simulations aimed at retrieving the QSO redshift from their observed colors. We first start with what we think to be a generic example of the broad band photometry, e.g., the one defined in the 1F system, and we show its limitations. Then we analyse the possible contributions of medium bands and we compare the efficiency of the 1F, 2A and 3G systems.

## 3.1 The (1F) broad band photometry

Figure 1 shows the two color-color diagrams which can be derived from the 1F broad band photometric system. The (F33b-F45b) vs (F45b-F63b) color-color diagram is typical of a (U-B) vs (B-R) one. The following generic features can be noted:

1. For $z_q \leqslant 2$, QSOs can easily be identified by their UV excess from stars except the white dwarfs, which constitute the traditional contaminant.

2. For $2.2 < z_q < 3.5$, QSOs cannot be distinguished from main sequence stars. This is a generic source of incompleteness in QSO catalogs selected from broad band photometry.

3. For $z_q > 4$, the QSO tracks are far from the stellar locus but they depend on the exact amount of absorption encountered along the line-of-sight (see the diverging tracks for $z > 2.2$ in Figure 1a).

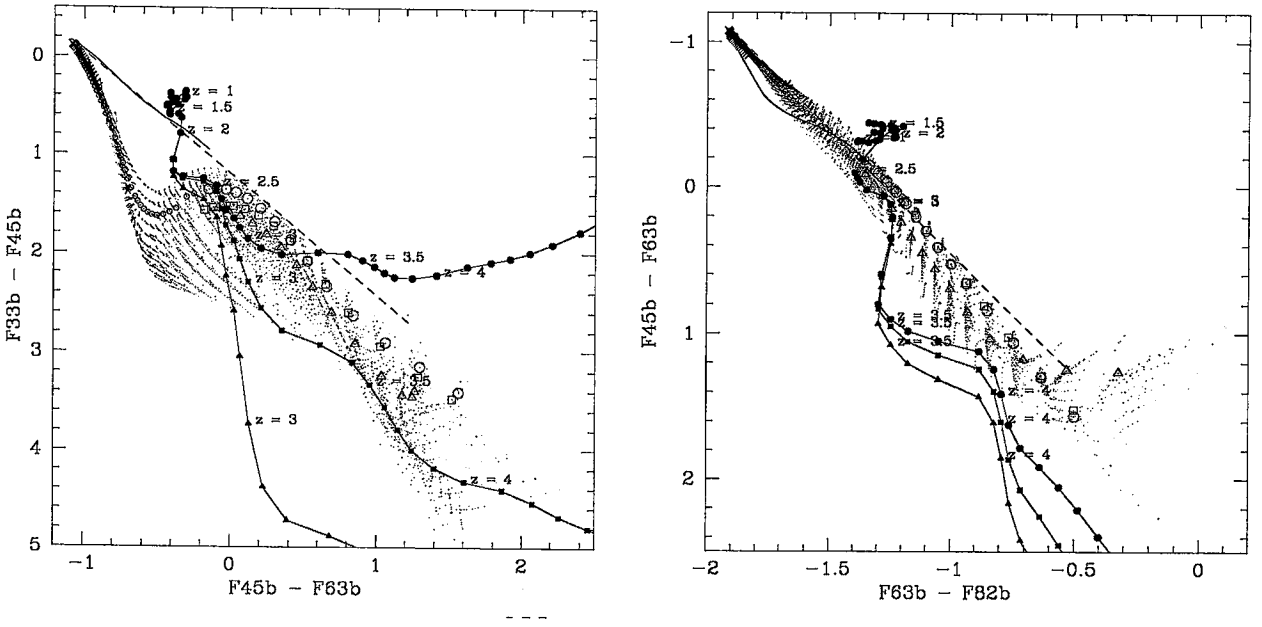


Figure 1: Color-color diagrams in the 1F broad band photometric system. The different tracks with filled symbols correspond to QSO colors ($\Delta z = 0.1$) with increasing absorption: model 1 (circles), 2 (squares) and 3 (triangles). Each small dot represents one Kurucz atmosphere model with [Fe/H] $> -3$. Open symbols select the stellar contaminants: cold halo main sequence (large circles), disk cold main sequence (triangles), cold halo giants (squares), subdwarf OB (crosses); small circles represent the unpopulated hot main sequence. The continuous line corresponds to the white dwarfs locus and the dashed line traces the theoretical locus of black bodies.

These features are qualitatively summarized in Figure 2. It is easy to note that the minimum distance between the QSO and the main sequence stellar locus in the 3 dimensional broad band color space shows a sharp decrease if $z_q > 2.2$. The subsequent increase is model-dependent. As a consequence (see also item 3 above), it is necessary to progressively drop the bluest indices when defining the color signature of the higher redshift QSOs. For these objects, the measured fluxes in the blue bands are also much lower and the photometric errors are very large.

The redshift of QSOs is a key-information for any study on their luminosity function or on the large scale structure and also for all possible gravitational lensing applications. In principle, it can be retrieved from the GAIA photometric measurements. How efficient are the broad band colors? In order to answer this question, we simulated QSO colors for different redshifts according to our model, then we added a gaussian noise on the basis of the expected magnitude uncertainties for a quasar with $V = 20$ and $z_q = 2$. (For each band, the uncertainty has been derived from Figure 8.8 in the GAIA Study Report and from the magnitude difference in the $V$ band between a G2V star and the QSO for a given flux in the respective filters). Finally, the redshift of the QSO is obtained from an approximate fit of the simulated colors with the QSO theoretical colors. The results and their dispersion obtained from 50 simulations are shown in

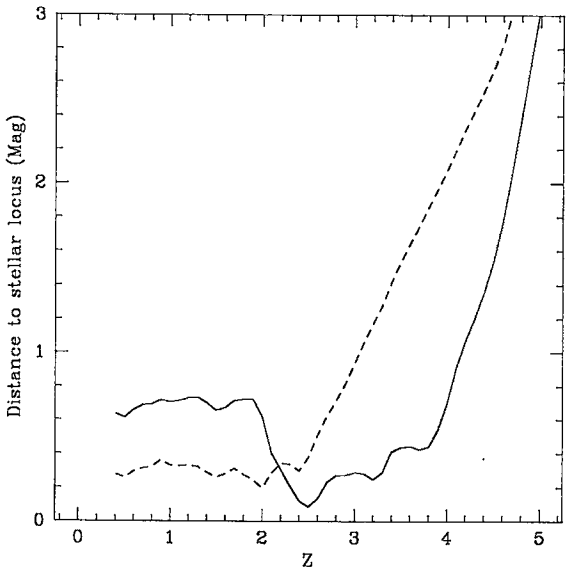


Figure 2: Shortest distance between the QSO color and the stellar locus defined by the halo main sequence stars (full line) and the white dwarfs (dashed line), in the 3 dimensional space of the 1F broad band system.

Figure 3. The error on the photometric redshift amounts to more than $\sigma_{z_q} = 0.5$ for $z_q \leqslant 1.5$; this is due to the degeneracy of the QSO colors in that redshift range, as seen in Figure 1. Then the accuracy is very good (but the QSO colors are close to stellar colors for $z_q \geqslant 2.2$). The behaviour at high redshift results from the lack of constraints, since only one color index is then independent of absorption for $z_q > 3$.

## 3.2 The medium band system

GAIA photometry in the medium band filters could potentially improve the situation by:

1. Removing the color degeneracy between stars and QSOs with $2 < z_q < 3.5$ thanks to a better sensitivity to the $Ly_\alpha$ emission line. This simultaneously requires a good spectral coverage between 3600Å and 5500Å and a bandwidth comparable to the $Ly_\alpha$ width, i.e. $\sim 75 \times (1+z)$Å.

2. Removing the dependence on the absorption model at high $z$ by adding red filters with $\lambda_c > 6000\mathring{A}$.

3. Increasing the accuracy on the determination of the photometric redshift.

Figure 4 shows the medium band transmission curves of the three photometric systems proposed for GAIA, superposed over the spectrum of a quasar at redshift $z_q = 2.8$. It is straightforward that the 2A photometric system should be excluded on the basis of the above

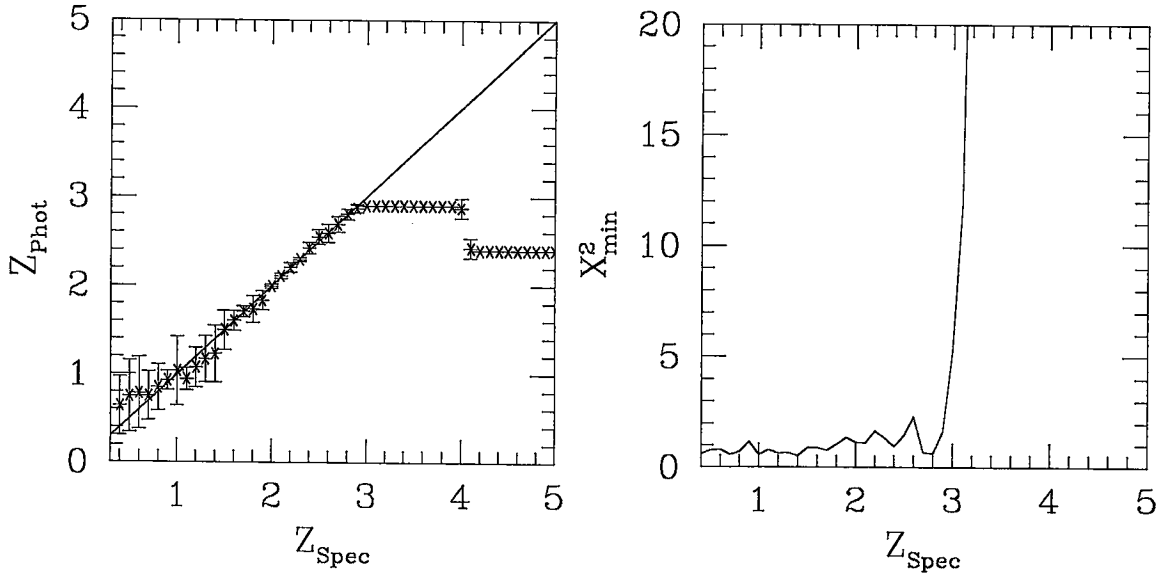


Figure 3: Photometric redshift as a function of spectroscopic redshift in the 1F broad band photometric system (left), for a QSO with $V = 20$. Error bars are $1\sigma$ dispersions from 50 simulations. The minimum $z_{Spec}$ is 0.4 because of the limited wavelength coverage of the composite template. The right panel shows the corresponding minimum $\chi^2$.

arguments: the spectral coverage is not good enough to follow the $Ly_\alpha$ line for $2 < z_q < 3.5$. Moreover, the bandwidth is *narrower* than the width of the $Ly_\alpha$ line, which translates in a very low integrated flux. At first glance, the 1F and 3G look more or less equivalent, with a better wavelength coverage in the 1F system and a better match to the $Ly_\alpha$ width in the 3G system.

In Figure 5, we present two typical color-color diagrams in the 1F system. F47n-F51n vs F51n-F57n illustrates the increased sensitivity to the $Ly_\alpha$ line at redshifts in the range $2 < z_q < 3.5$; F57n-F67n vs F67n-F75n does not only show that quasar with $z_q > 4$ have colors different from stars but also that these are *independent* of the absorption model for $z_q \leqslant 4.6$.

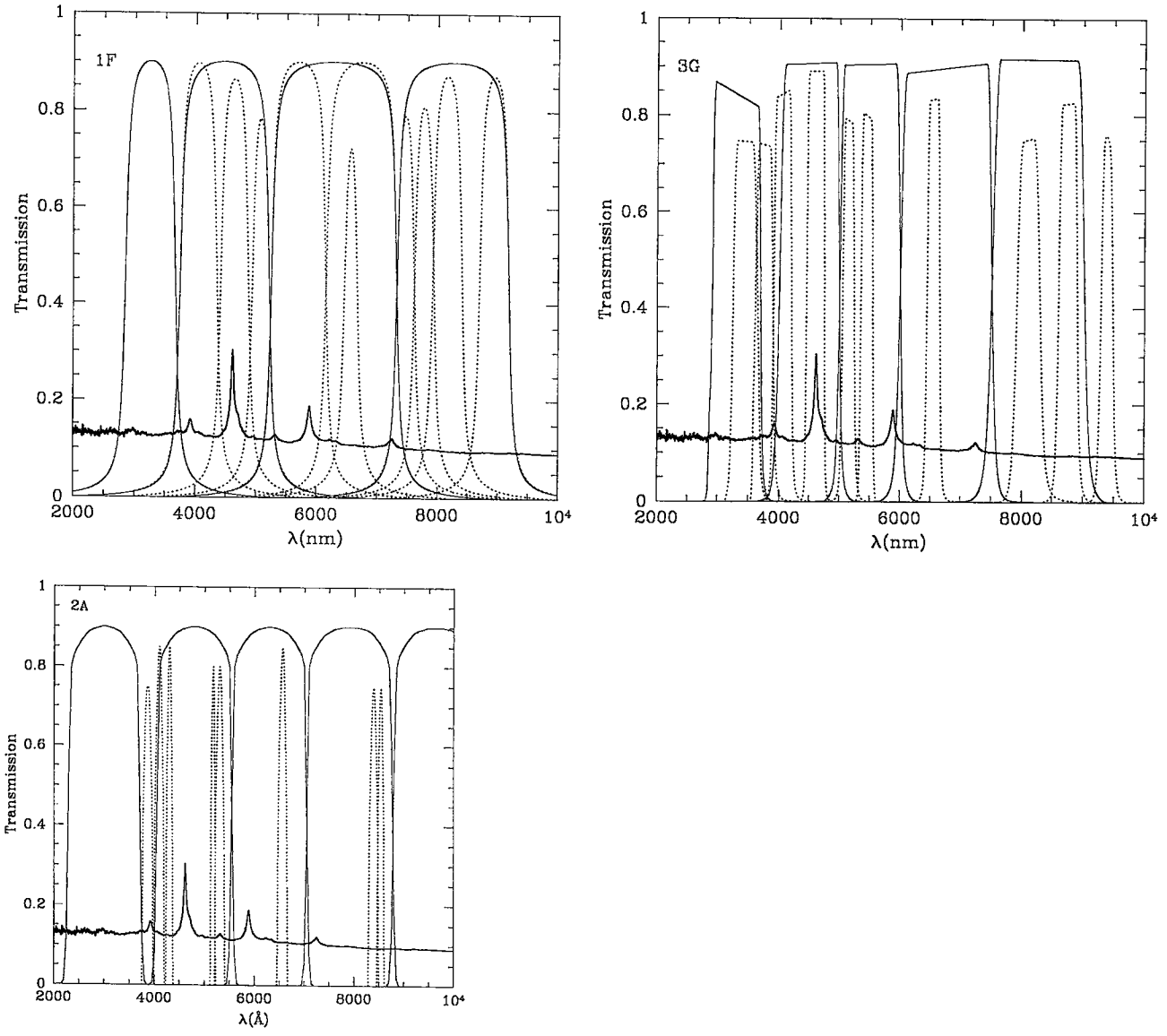


Figure 4: Medium band transmission curves for the 1F (top left), 3G (top right) and 2A (bottom left) photometric systems. The thick line represents the spectrum of a QSO with $z_q = 2.8$.

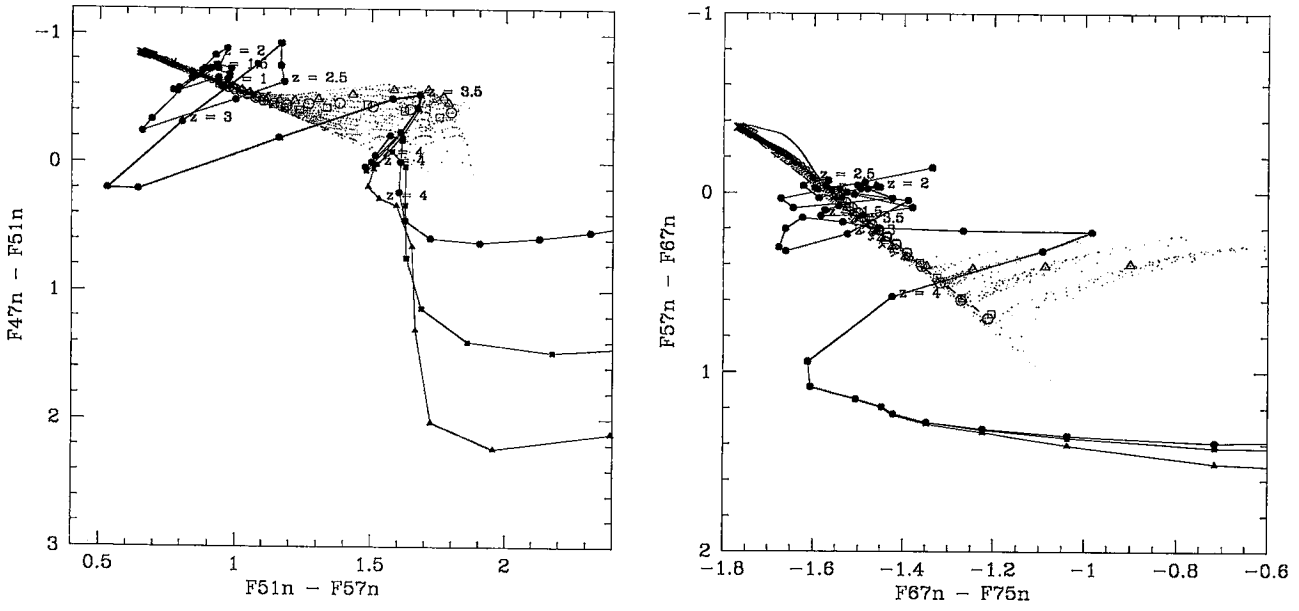


Figure 5: Two examples of color-color diagrams in the 1F medium band system (see text). Same symbols as in Fig. 1.

Table 3: Color indices insensitive to absorption in the 1F system, as a function of the redshift interval of the quasar.

| z | 33-45 | 45-63 | 63-82 | 33-41 | 41-47 | 47-51 | 51-57 | 57-67 | 67-75 | 75-78 | 78-82 | 82-89 |
|---|---|---|---|---|---|---|---|---|---|---|---|---|
| 4.2-5.0 | | | X | | | | | X | X | X | X | X |
| 3.5-4.2 | | | X | | | | X | X | X | X | X | X |
| 3.0-3.5 | | | X | | | X | X | X | X | X | X | X |
| 2.5-3.0 | | X | X | | X | X | X | X | X | X | X | X |
| 0.0-2.5 | X | X | X | X | X | X | X | X | X | X | X | X |

Table 4: Color indices insensitive to absorption in the 3G system, as a function of the redshift interval of the quasar.

| z | ug-bg | bg-vg | vg-rg | rg-ig | u-p | p-v | v-b | b-z | z-y | y-s | s-p1 | p1-p2 | p2-p3 |
|---|---|---|---|---|---|---|---|---|---|---|---|---|---|
| 4.5-5 | | | | | | | | | | X | X | X | X |
| 3.8 -4.5 | | | X | X | | | | | X | X | X | X | X |
| 3.2-3.8 | | | X | X | | | | X | X | X | X | X | X |
| 2.8-3.2 | | X | X | X | | | X | X | X | X | X | X | X |
| 2.5-2.5 | | X | X | X | | X | X | X | X | X | X | X | X |
| 0.0- 2.5 | X | X | X | X | X | X | X | X | X | X | X | X | X |

Tables 3 and 4 indicate, as a function of the redshift interval, which color indices are kept in the following analysis.

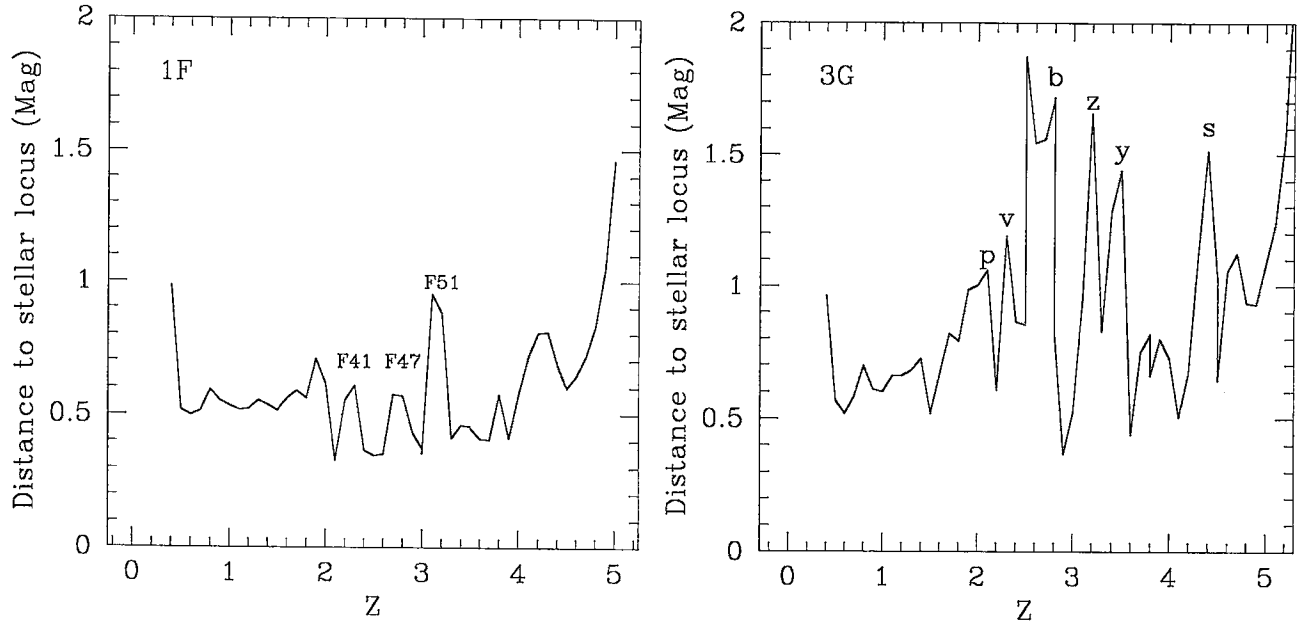


Figure 6: Shortest distance between the QSO color and the stellar locus defined by the halo main sequence stars, in the 1F (left) and 3G (right) medium band systems. The signature of $Ly_\alpha$ in some filters is identified by the filter name.

The quasars at any redshift may easily be identified from the stars by using their photometry in medium bands, either with the 1F or with the 3G system. This is qualitatively shown in Figure 6. Quantitatively, the photometric redshift can be retrieved with both photometric systems, as it is illustrated in Figure 7; the stars and white dwarfs can be discriminated by the high value of their minimum chi square. However, the slope of the continuum of a real QSO may differ from that of the composite template. In that case, although the photometric error in the 3G system is estimated to be 50 to 120% larger than in the 1F system at $V = 20$, the former is more robust than the latter. Indeed, the larger bandwidths of the 1F filters make this system more sensitive to the exact continuum slope while the 3G system is more sensitive to the flux in the emission lines. Figure 8 shows the estimated photometric redshift as a function of the true redshift in both photometric systems, for a QSO whose continuum spectrum is a power law with $\alpha = -0.32$ for $\lambda > 1025\mathring{A}$ (to be conservative, the estimated photometric errors in the 3G system have been multiplied by a factor two).

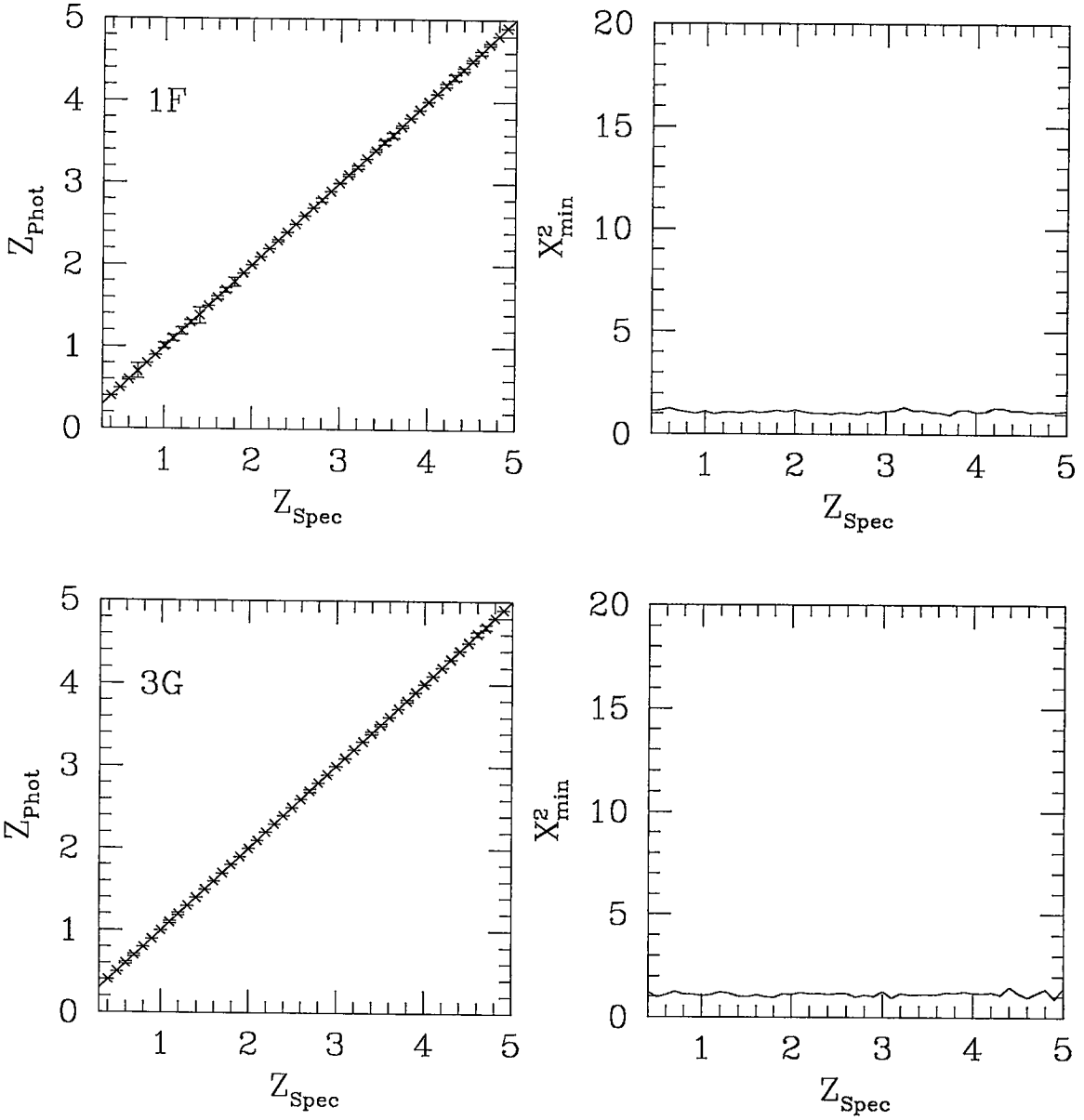


Figure 7: Photometric redshift as a function of spectroscopic redshift in the 1F (top) and 3G (bottom) system for a QSO with $V = 20$; see caption Fig. 3.

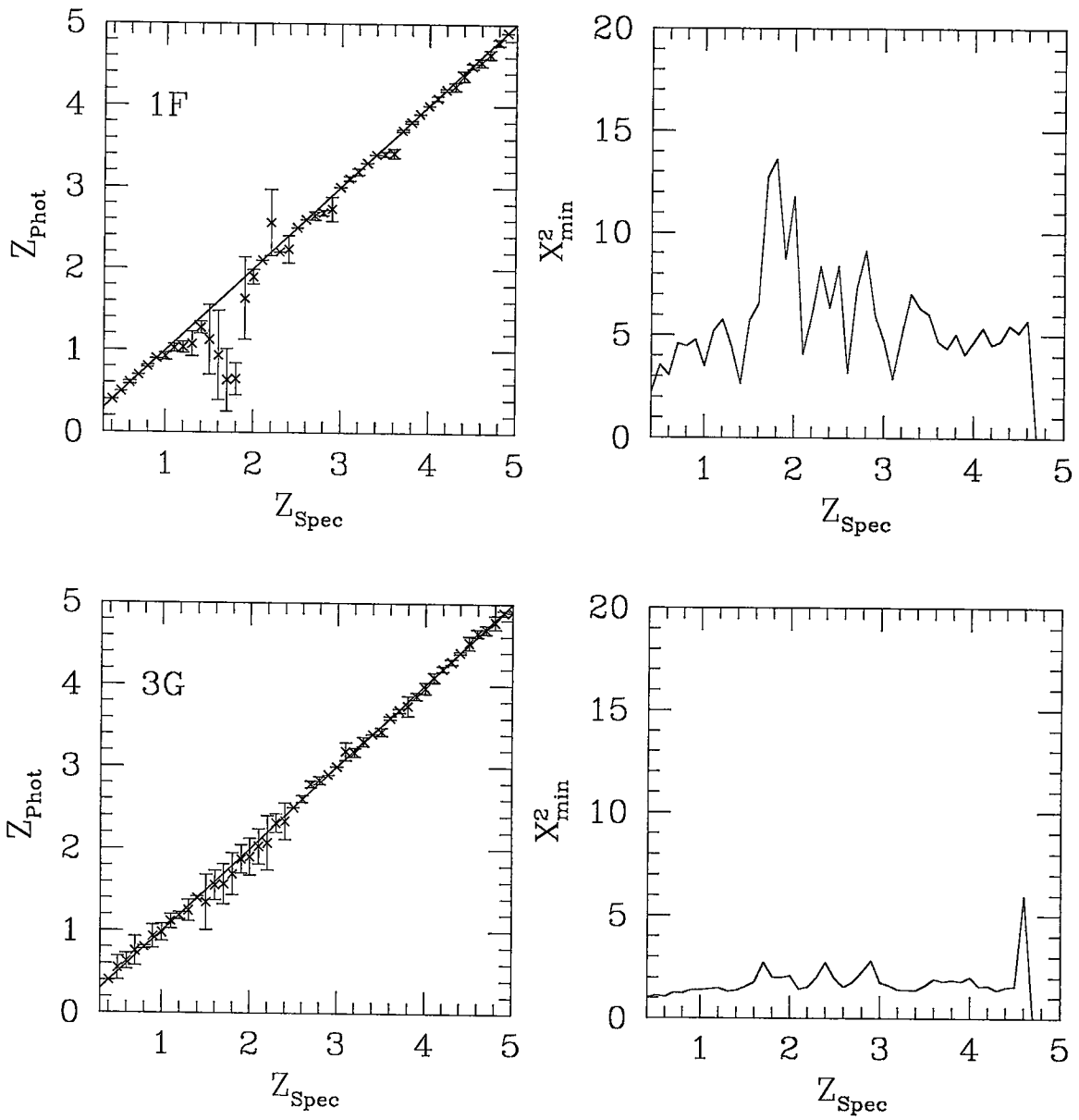


Figure 8: Photometric redshift as a function of spectroscopic redshift in the 1F (top) and 3G (bottom) system, for a QSO with $V = 20$; the simulated QSO continuum spectrum is a power law with $\alpha = -0.32$ for $1025 \leqslant \lambda \leqslant 8000\mathring{A}$.

# 4 Conclusions

As a conclusion of this preliminary study, we may state that medium band filters in both the 1F and 3G photometric systems are extremely useful in order to identify QSOs and derive their photometric redshift. In those systems, QSOs with V $\leqslant$ 20 can indeed be distinguished at any redshift ($z_q \leqslant 5$) from stars, independently of the amount of absorption by gas-clouds located along the line-of-sight, by using red colors at high redshift. The 3G system is slightly better than the 1F to determine the photometric redshift, in the sense that it is less sensitive to the exact slope of the continuum of the QSO spectrum. The 2A photometric system is not suitable at all, mainly because of its poor wavelength coverage and because the filters are very narrow. Therefore:

$$\Rightarrow \mathbf{3G} \gtrsim \mathbf{1F} \gg \mathbf{2A}$$

Finally, besides this photometric aspect, we would like to recall that it is important to get color information for fainter ($20 < V < 23$) pointlike objects located between a few tenths and at least 3 arcsec apart from the QSOs in order to identify *all* the multiply imaged QSOs lensed by normal galaxies. GAIA would then provide us with the most *complete*, all-sky census of the *brightest* multiply imaged QSOs, which are the best targets for subsequent astrophysical and cosmological applications, such as the study of the matter distribution and of the extinction law in distant galaxies, the determination of the scaling factor of the Universe from time delay measurements and the statistical estimation of the cosmological density and the cosmological constant.

On the other hand, high angular resolution morphological information on the QSOs in white light from the Astro Sky Mapper should allow the detection of multiply imaged QSO candidates with very small angular separations (typically $< 0.3$"), either lensed by objects with subgalactic masses or produced when the source is located very close to a caustic. Moreover, the host galaxy of the least distant quasars could also be evidenced in this way.

# References


[1] Cristiani, S., Vio, R., 1990, A&A 227, 385

[2] Francis, P.J., Hewett, P.C., Foltz, C.B. et al. 1991, ApJ 373, 465

[3] Giallongo E., Trevese, D., 1990, ApJ 353, 24

[4] Irwin, M., McMahon, R.G., Hazard C., 1991, in: Crampton D. (ed) The Space Distribution of Quasars, ASP Conf. Ser. 21, 117

[5] Koester, D., 1999 (private communication)

[6] Kurucz, R.L., 1992 in: Barbuy, B., and Renzini A. (eds.) The stellar populations of galaxies, IAU Symp. 149. Dordrecht, Kluwer Acad. Pub. p.225

[7] Møller, P., Jakobsen, P., 1990, A&A 228, 299

[8] Møller, P., Warren, S.J., 1991, in: Crampton D. (ed) The Space Distribution of Quasars, ASP Conf. Ser. 21, 96

[9] Warren, S.J., Hewett, P.C., Osmer, P.S., 1994, ApJ 421, 412

[10] Zheng, W., Kriss, G.A., Telfer R.C. et al. 1997, ApJ 475, 469

[11] Zuo, L., Lu, L., 1993, ApJ 418, 601